

UT-04-27
hep-th/0410138
October 2004

On String Junctions in Supersymmetric Gauge Theories

Yosuke Imamura*

Department of Physics, University of Tokyo, Tokyo 113-0033, Japan

Abstract

We study junctions consisting of confining strings in $\mathcal{N} = 1$ supersymmetric large N gauge theories by means of the gauge/gravity correspondence. We realize them as D-brane configurations in infrared geometries of the Klebanov-Strassler (KS) and the Maldacena-Núñez (MN) solutions. After discussing kinematics associated with the balance of tensions, we compute energies of baryon vertices numerically. In the KS background, baryon vertices give negative contributions to energies. The results for the MN background strongly suggest that energies of baryon vertices exactly vanish just like the case of supersymmetric (p, q) -string junctions. We find that brane configurations in the MN background have a property similar to the holomorphy of the M-theory realization of (p, q) -string junctions. With the help of this property, we analytically prove the disappearance of the energies of baryon vertices in the MN background.

*E-mail: imamura@hep-th.phys.s.u-tokyo.ac.jp

1 Introduction

The gauge/gravity correspondence[1, 2, 3] relates five-dimensional gravitational backgrounds to four-dimensional field theories on the boundaries of the five-dimensional spacetimes. The extra dimension r is related to the energy scales of field theories via red-shift (warp) factors depending on r . The five-dimensional spacetimes are in general accompanied by compact internal spaces. The structure of these higher-dimensional spacetimes reflect non-perturbative properties of their dual field theories. A lot of gravity duals of various field theories have been constructed in string theory as near horizon geometries of branes on which gauge theories are realized.

Different particles in boundary field theories are identified with various objects in string theory. Spectra of glueballs[4, 5, 6, 7], mesons[8, 9, 10, 11, 12, 13, 14] and (di-)baryons[15, 16, 17, 18, 19], and interactions among them[20, 21, 13] have been studied in different ways. In [22], the duality is used to explain the extremely narrow decay width of pentaquark baryons[23, 24].

Hadrons in $SU(N)$ gauge theories are bound states of (anti-)quarks belonging to the (anti-)fundamental representation. In order to introduce such quarks and antiquarks, we need to put flavor D-branes in the dual gravity background[25]. Quarks are identified with endpoints of open strings on the flavor branes, and hadrons are constructed by connecting them. For example, a meson consisting of a quark and an antiquark is realized as an open string stretched between two flavor branes on the gravity side as (a) in Figure 1.

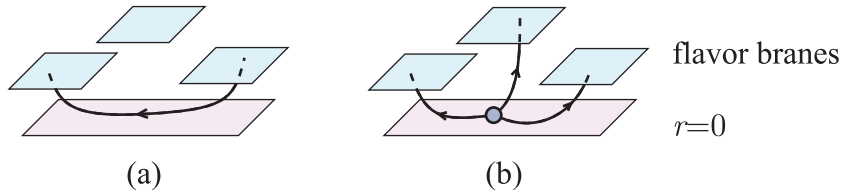


Figure 1: A meson configuration (a) and a baryon configuration (b)

Among a lot of states in a meson spectrum, some low-lying states of pseudo scalar and vector mesons are identified with string modes representing fluctuations of the flavor branes and gauge fields on them. Masses of such modes are examined in [9, 10], and the existence of localized modes with mass gap is found.

By contrast, Regge trajectories of higher-spin mesons can be analyzed as semi-classical spinning strings in curved backgrounds[9, 14]. In general, it is difficult to solve the motion of strings completely, and the Born-Oppenheimer approximation is often used to simplify problems. In this method, a quark-antiquark potential is computed as an energy of a string with fixed end points[26, 27], and then, motion of the endpoints (the quark and the antiquark) is solved as a potential problem. If the distance L between a quark and an antiquark is large, the L -dependence

of the potential energy is in general expanded as

$$E_{q\bar{q}} = TL + M_q + M_{\bar{q}} + \mathcal{O}(L^{-1}) \quad (1)$$

for large L . The coefficient T of the first term is the tension of the confining string between the quark and the antiquark. From the gravity point of view, the first term is interpreted as the contribution of the tension of a fundamental string going at $r = 0$ because fundamental strings tend to approach $r = 0$ due to the gravitational force. Thus, T is obtained as the product of the redshift (warp) factor and the proper tension of fundamental strings. In general, confining strings can be bound states of elementary confining strings. The tension of such strings depends on the number of constituent elementary strings non-linearly. This property is reproduced on the gravity side[28] by taking account of deformation of fundamental strings to D-branes puffed up in internal spaces by the Myers' effect[29]. The second and the third terms in (1) independent of L are interpreted as self-energies of the quark and the antiquark. These can be evaluated by analyzing the catenary profile of the string near the flavor D-branes.

A baryon is constructed by connecting flavor D-branes by N open fundamental strings with the same orientation. In order to join these strings without being against the conservation law of the fundamental string charge, we have to introduce a baryon vertex at the joint[15, 5]. ((b) in Figure 1) It is a certain D-brane wrapped on a non-trivial cycle in the internal space. In general, strings stretched between a baryon vertex and a flavor D-brane could be bound, and the number of confining strings meeting at a vertex can be smaller than N .

Let us consider the potential among quarks in a baryon in the spirit of the Born-Oppenheimer approximation.[16] If the length of each confining string is large, the energy of a baryon configuration is given by

$$E_{\text{baryon}} = \sum_i T_i L_i + \sum_i M_i + E_{\text{vertex}} + \mathcal{O}(L_i^{-1}), \quad (2)$$

where L_i and T_i are the length and the tension of the i -th confining string, and M_i represents the self-energy of the quark at the end of the i -th confining string. The third term E_{vertex} is a new contribution which is absent in meson energies. Naively, this contribution can be evaluated by multiplying the tension T of the D-brane which the baryon vertex is made of, the volume V of the cycle which the D-brane is wrapped on, and the warp factor. Although this does not give an exact result because of the deformation of the brane by the string tension[17, 18], we expect that a vertex gives some positive contribution of the order of $TV \times (\text{warp factor})$. The purpose of this paper is to compute this quantity in numerical and analytic ways.

This paper is organized as follows. In the next section, we give our setup. The junctions are realized as D3-brane configurations embedded in a six-dimensional geometry. In Section 3, we briefly review the result of [28] about the confining

string tension, and study the kinematics of junctions associated with the tension balance. In section 4, as a preparation of the following computations, we rewrite brane configurations as two-dimensional surfaces in a certain four-dimensional target space by assuming a certain symmetry. Numerical computations are made in Section 5, and we give some analytic results in Section 6. We conclude in Section 7. In the appendix, we briefly explain how the electric fields on D3-branes are treated in the numerical computations.

2 D3-branes in the infrared geometry

We use two different classical solutions in type IIB supergravity as background spacetimes dual to $\mathcal{N} = 1$ supersymmetric confining gauge theories. One is the Maldacena-Núñez (MN) solution[30, 31], and the other is the Klebanov-Strassler (KS) solution[32, 33, 34].

The MN solution is the near horizon geometry of N coincident D5-branes wrapped on a two-cycle in a non-compact Calabi-Yau manifold. This is expected to be the gravity dual to the $\mathcal{N} = 1$ $SU(N)$ pure Yang-Mills theory. This theory has only two parameters: the size of gauge group N and the confinement scale Λ_{QCD} .

The KS solution can be interpreted as the near horizon geometry of coincident $N+k$ D5-branes and k anti D5-branes wrapped on a two-cycle. The corresponding boundary field theory is an $\mathcal{N} = 1$ $SU(N+k) \times SU(k)$ gauge theory with bifundamental chiral multiplets. The number k depends on the energy scale. As the energy is decreased, k also decreases by the cascade phenomenon[33]. In the brane picture, this can be regarded as a kind of pair annihilation of D5-branes and anti D5-branes. At a very low energy, all the anti D5-branes disappear with the same number of D5-branes to leave N D5-branes. Thus, the boundary theory of the KS solution behaves like the $\mathcal{N} = 1$ $SU(N)$ supersymmetric Yang-Mills theory in the low energy limit. In addition to N and Λ_{QCD} , this theory has another parameter \bar{g} defined by $\bar{g}^{-2} = g_1^{-2} + g_2^{-2}$ where g_1 and g_2 are the gauge coupling constants of $SU(N+k)$ and $SU(k)$, respectively. Although g_1 and g_2 run with the energy scale individually, \bar{g} is a renormalization invariant parameter. This is related to the string coupling constant g_{str} , which is constant in the KS solution, by

$$\bar{g}^2 = 4\pi g_{\text{str}}. \quad (3)$$

Corresponding to the similarity of the low-energy behaviors of the two gauge theories, two classical solutions have similar structure. They are warped products of a five-dimensional manifold with coordinates (x^μ, r) and an internal space with the topology of $\mathbf{S}^2 \times \mathbf{S}^3$. The \mathbf{S}^2 shrinks to a point at $r = 0$ while \mathbf{S}^3 keeps non-zero size everywhere. The infrared (IR) dynamics of the field theories is reflected by the structure near the centers of the classical solutions. For both the MN and the KS solutions, the metric of $r = 0$ subspace relevant to the IR dynamics is

given by

$$ds^2 = R^2(\eta_{\mu\nu}dy^\mu dy^\nu + d\Omega_3^2), \quad (\mu, \nu = 0, 1, 2, 3) \quad (4)$$

where $d\Omega_3^2$ is the metric of unit \mathbf{S}^3 . We refer to this as IR geometry. The size N of the low-energy gauge group $SU(N)$ of the boundary gauge theories is determined by the R-R 3-form flux flowing through the \mathbf{S}^3 . Namely, the integral of the R-R 3-form field strength G_3 over the non-trivial 3 cycle gives N .

$$N = \oint_{\mathbf{S}^3} G_3. \quad (5)$$

Boundary theories of the MN and the KS solutions include only adjoint and bifundamental fields. In order to introduce fundamental quarks in these theories, we need flavor D-branes. Because the classical solutions can be regarded as the near horizon geometries of D5-branes wrapped on \mathbf{S}^2 , supersymmetric flavor branes should be D7-branes intersecting with the \mathbf{S}^2 at points according to the $\#DN=4$ rule. Hadrons are constructed by connecting these branes by fundamental strings joined by baryon vertices. We assume the lengths of strings are large and focus on the vicinity of baryon vertices, which are located at the bottom ($r = 0$) of the classical solutions due to the gravitational force. We will not discuss the effect of the endpoints of strings on the D7-branes.

In the case of the MN and the KS backgrounds, baryon vertices are D3-branes wrapped on \mathbf{S}^3 [35, 32, 36], and fundamental strings in the IR geometry are puffed up to D3-brane tubes with section \mathbf{S}^2 [28] due to the existence of the G_3 flux by the Myers' effect[29]. Therefore, junctions of confining strings are dual to D3-branes with electric flux on them embedded in the IR geometry.

The magnetic flux on D3-branes carries the charge of D-strings, which in the KS solution have been recently identified with axionic strings[37]. We will not discuss them in this paper.

The action of a D3-brane in the IR geometry described by the metric (4) and the R-R flux (5) is

$$S = -T_{D3} \int d^4\sigma \sqrt{-\det \left(g_{ab} + \frac{2\pi}{T_{\text{str}}} F_{ab} \right)} + 2\pi \int F_2 \wedge C_2, \quad (a, b = 0, 1, 2, 3) \quad (6)$$

where $T_{\text{str}} = 1/(2\pi\alpha')$ and $T_{D3} = 1/((2\pi)^3\alpha'^2 g_{\text{str}})$ are the tensions of fundamental strings and D3-branes, respectively. C_2 is the R-R two-form potential and $G_3 = dC_2$. When a confining string consisting of n elementary strings is realized as a D3-brane configuration with the topology of $\mathbf{R}^2 \times \mathbf{S}^2$, the integer n is defined as the fundamental string charge carried by the D3-brane. The fundamental string current is derived from the action (6) by differentiating it with respect to the NS-NS two-form potential B_2 . (In the derivation of the current, F_2 should be regarded as the B -gauge invariant field strength $dA_1 + B_2$. Once we have obtained the current, we set $B_2 = 0$.) n is given by integrating the current as

$$n = \oint_X dS_a D^a - \oint_X C_2 = \oint_X dS_a D^a - \int_Y G_3, \quad (a = 1, 2, 3) \quad (7)$$

where X is a non-trivial 2-cycle in the D3-brane worldvolume and Y is a 3-disk with the boundary $\partial Y = X$. The flux density D^a in (7) is defined by

$$D^a = \frac{1}{2\pi} \frac{\delta S_{\text{BI}}}{\delta F_{0a}}, \quad (a = 1, 2, 3) \quad (8)$$

Note that we use S_{BI} , the Born-Infeld part of the action (6), to define D^a . The flux density defined in this way is invariant under gauge transformations of the R-R 2-form potential C_2 . Due to the ambiguity of the choice of Y in \mathbf{S}^3 , n is defined only mod N . n is a conserved charge and is not changed by continuous deformations of the brane.

We define a “flux angle” θ^f by

$$\theta^f = \pi \frac{n}{N}, \quad (9)$$

for later use. We fix the mod- π ambiguity of θ^f by $0 < \theta^f < \pi$. Because the sum of charges n of strings meeting at a baryon vertex must be a multiple of N , the sum of corresponding flux angles is a multiple of π . If the number of branches is three, the sum can be π or 2π . These two are essentially the same via the charge conjugation $\theta^f \rightarrow \pi - \theta^f$. If the number of branches is larger than three there are more than two genuinely different cases as we will see later explicitly for four-string junctions.

To clarify the dependence of the action (6) on the parameters R and N , we factor out these parameters from the induced metric and the R-R 3-form flux by

$$g_{ab} = R^2 \tilde{g}_{ab}, \quad G_3 = \frac{N}{2\pi^2} \omega_3, \quad (10)$$

where ω_3 is the volume form of \mathbf{S}^3 so normalized that its integral over \mathbf{S}^3 gives $\oint_{\mathbf{S}^3} \omega_3 = 2\pi^2$, the volume of the unit 3-sphere. At the same time, we introduce a rescaled field strength \tilde{F}_2 and the corresponding potential \tilde{A}_1 by

$$F_2 = \frac{R^2 T_{\text{str}}}{2\pi} \tilde{F}_2, \quad A_1 = \frac{R^2 T_{\text{str}}}{2\pi} \tilde{A}_1. \quad (11)$$

The D3-brane action rewritten in terms of these rescaled fields is

$$\tilde{S} = - \int d^4\sigma \sqrt{-\det(\tilde{g}_{ab} + \tilde{F}_{ab})} + \rho \int \tilde{A}_1 \wedge \omega_3, \quad \rho = \frac{NT_{\text{str}}}{2\pi^2 R^2 T_{\text{D3}}}. \quad (12)$$

Here we changed the normalization of the action by $S = T_{\text{D3}} R^4 \tilde{S}$. This does not affect the classical equations of motion we are interested in. The dimensionless quantity ρ is a unique parameter of this rescaled action. It is related to the parameter b used in [28] by $\rho = 2/b$. It is also convenient to notice the relation

$$\frac{2}{\rho} = b = \frac{R^2}{R_{\text{D5}}^2}, \quad (13)$$

where $R_{D5} = (N\alpha'g_{\text{str}})^{1/2}$ is the radius of \mathbf{S}^3 near the horizon of N coincident flat D5-branes in the flat Minkowski background. Because the MN solution can be regarded as the near horizon geometry of D5-branes wrapped on \mathbf{S}^2 , the radius R is identical to R_{D5} , and $b = 1$. On the other hand, b of the KS solution is modified due to the existence of anti D5-branes, and its numerical value is $b = 0.932660368\cdots$ [33, 28]. From the action (12), we can regard the dimensionless parameter ρ as a charge density coupled to the gauge field \tilde{A}_1 .

In this paper, we only consider static configurations, and always omit the time direction in the following. By the term “worldvolume” we mean a time slice of a whole worldvolume.

Instead of D^a defined by (8), we use the rescaled flux density and its Hodge dual defined by

$$\tilde{D}^a = \frac{\delta \tilde{S}}{\delta \tilde{F}_{0a}} = \frac{2\pi^2 \rho}{N} D^a, \quad \tilde{D}_2 = \frac{1}{2} \sqrt{\det \tilde{g}_{ab}} \epsilon_{abc} D^a d\sigma^b \wedge d\sigma^c, \quad (a, b, c = 1, 2, 3). \quad (14)$$

The relation (7) rewritten in terms of the flux angle and the rescaled flux density is

$$2\pi\rho\theta^f = \oint_X \tilde{D}_2 - \rho \int_Y \omega_3. \quad (15)$$

This is the integral form of the Gauss law constraint

$$d\tilde{D}_2 = \rho\omega_3|_{\text{brane}}, \quad (16)$$

where $\omega_3|_{\text{brane}}$ is the pull-back of ω_3 to the D3-brane worldvolume.

The energy of a D3-brane is given by $E = T_{D3}R^3\tilde{E}$ where \tilde{E} is the rescaled energy

$$\tilde{E} = \int d^3\sigma \sqrt{\det \tilde{g}_{ab}} \sqrt{1 + \tilde{g}_{ab}\tilde{D}^a\tilde{D}^b}, \quad (a, b = 1, 2, 3). \quad (17)$$

The shape of a D3-brane and the electric flux density on it should be determined so that they minimize this energy.

In the following sections, we will use only rescaled quantities like \tilde{E} , \tilde{D}^a and \tilde{g}_{ab} . In the rest of this section, let us summarize the relations between these dimensionless quantities and dimensionful ones in boundary field theories. From the definition of the rescaled quantities \tilde{S} and \tilde{g}_{ab} , we can determine the relations of rescaled energies and tensions to original ones. To translate them to quantities in boundary field theories, we should also take account of the warp factor W , which determine the ratio between energies in the IR geometry and ones in the boundary field theories. As a result, we obtain

$$E_{\text{vertex}}^{(\text{FT})} = WT_{D3}R^3\tilde{E} = \left(\frac{W}{\alpha'^{1/2}}\right) \frac{bN^{3/2}g_{\text{str}}^{1/2}}{(2\pi)^3} \tilde{E}_{\text{vertex}}, \quad (18)$$

$$T^{(\text{FT})} = W^2 T_{D3} R^2 \tilde{T} = \left(\frac{W}{\alpha'^{1/2}}\right)^2 \frac{bN}{(2\pi)^3} \tilde{T}, \quad (19)$$

where $\tilde{E}_{\text{vertex}}$ and \tilde{T} are the energy of a baryon vertex and a confining string tension appearing in the following sections, and $E_{\text{vertex}}^{(\text{FT})}$ and $T^{(\text{FT})}$ are the corresponding quantities in the boundary field theories.

The confinement scale Λ_{QCD} in the boundary gauge theories can be defined by $T^{(\text{FT})} \sim \Lambda_{\text{QCD}}^2$. Thus, up to numerical factor,

$$\Lambda_{\text{QCD}} \sim \frac{W}{\alpha'^{1/2}}. \quad (20)$$

(Here we used the tension of an elementary confining string $\tilde{T} \sim N^{-1}$.) Then, the energy of a baryon vertex is rewritten as

$$E_{\text{vertex}}^{(\text{FT})} \sim \Lambda_{\text{QCD}} N^{3/2} g_{\text{str}}^{1/2} \tilde{E}_{\text{vertex}}. \quad (21)$$

This depends on the string coupling constant g_{str} . In the KS case, g_{str} is related to the parameter \bar{g} by (3), and we obtain the following relation which includes only field theory variables.

$$E_{\text{vertex}}^{(\text{FT})} \sim \Lambda_{\text{QCD}} N^{3/2} \bar{g} \tilde{E}_{\text{vertex}}. \quad (22)$$

On the other hand, we have no parameter corresponding to g_{str} in the MN case. We will return to this problem in §6.

In the following sections we only use dimensionless quantities, and we omit tildes on rescaled variables.

3 Confining strings and their junctions

In this section we first briefly review how the tensions of confining strings are computed as energies of D3-branes following [28]. And then, we study the kinematics of junctions by considering the balance of tensions on vertices.

Let (x, y, z) be the three spatial coordinates on the boundary. Together with coordinates of the internal space \mathbf{S}^3 , we use the coordinates $(x, y, z, \theta, \phi, \psi)$ with the following metric.

$$ds^2 = dx^2 + dy^2 + dz^2 + d\theta^2 + \sin^2 \theta (d\phi^2 + \sin^2 \phi d\psi^2). \quad (23)$$

The ranges of the angular coordinates are

$$0 \leq \theta \leq \pi, \quad 0 \leq \phi \leq \pi, \quad 0 \leq \psi < 2\pi. \quad (24)$$

With this parameterization, the volume form of \mathbf{S}^3 is given by

$$\omega_3 = \sin^2 \theta \sin \phi d\theta \wedge d\phi \wedge d\psi. \quad (25)$$

The dual configuration of an infinitely long confining string is a D3-brane with the worldvolume $\mathbf{S}^2 \times \mathbf{R}$. We start with the ansatz

$$x = \sigma^1, \quad y = 0, \quad z = 0, \quad \theta = \theta^r, \quad \phi = \sigma^2, \quad \psi = \sigma^3. \quad (26)$$

The parameter θ^r is a constant representing the angular radius of $\mathbf{S}^2 \subset \mathbf{S}^3$. By the rotational symmetry, we can easily determine the flux density D^a as a function of θ^f and θ^r from (15). Its non-vanishing component is only D^x , and is given by

$$D^x = \frac{1}{b \sin^2 \theta^r} [\theta^f - (\theta^r - \sin \theta^r \cos \theta^r)]. \quad (27)$$

Substituting this into (17), we obtain the tension of a confining string.

$$T = \frac{dE}{dx} = 4\pi \sqrt{\sin^4 \theta^r + \frac{1}{b^2} (\theta^f - \theta^r + \sin \theta^r \cos \theta^r)^2}. \quad (28)$$

We should determine the angle θ^r as the minimum tension point. The condition $dT/d\theta^r = 0$ gives the relation between θ^f and θ^r .

$$\theta^r - (1 - b^2) \sin \theta^r \cos \theta^r = \theta^f. \quad (29)$$

If $0 \leq b^2 \leq 1$, this relation defines a one to one mapping between $0 \leq \theta^f \leq \pi$ and $0 \leq \theta^r \leq \pi$. The minimum tension is

$$T = 4\pi \sin \theta^r \sqrt{\sin^2 \theta^r + b^2 \cos^2 \theta^r}. \quad (30)$$

For the MN solution, (29) is immediately solved, and the tension (30) reduces to the simple form:

$$\theta^f = \theta^r, \quad T = 4\pi \sin \theta^f, \quad \text{for } b = 1. \quad (31)$$

On the other hand, the angle θ^r and the tension for the KS solution are obtained only numerically. Tensions and θ^r for some values of θ^f are shown in Table 1. These values will be used to compute the energies of baryon vertices later.

In both cases of the MN and the KS backgrounds, the tension depends on θ^f non-linearly. This non-linear dependence implies the formation of truly bound states and the absence of supersymmetry. Thus we cannot apply the method using killing spinors, which is useful to determine the baryon configuration in $\mathcal{N} = 4$ Yang-Mills theory[17], to configurations discussed in this paper.

Using the tension formula obtained above, let us consider kinematics of three and four-string junctions. We first discuss three-string junctions. The angles at which the strings meet are fixed by the requirement of the balance of the tensions on the vertex. If we define the angle θ_i^t as the opposite angle of the force vector of i -th string in the triangle consisting of three force vectors, the angle made by

Table 1: The angle θ^r and the tension T for several values of θ^f

θ^f	MN ($b = 1$)		KS ($b = 0.9326604$)	
	θ^r	T	θ^r	T
$\pi/12 = 0.261799$	0.261799	3.252416	0.298366	3.467446
$2\pi/12 = 0.523599$	0.523599	6.283185	0.583434	6.601513
$3\pi/12 = 0.785398$	0.785398	8.885766	0.849929	9.168758
$4\pi/12 = 1.047198$	1.047198	10.882796	1.099822	11.047175
$5\pi/12 = 1.308997$	1.308997	12.138181	1.338189	12.185588
$6\pi/12 = 1.570796$	1.570796	12.566371	1.570796	12.566371

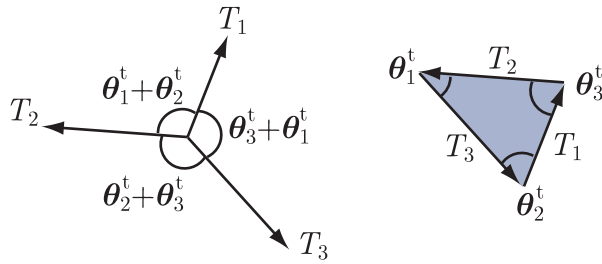


Figure 2: The balance of three tensions.

the i -th and the j -th strings is $\theta_i^t + \theta_j^t$. (Figure 2) If the tensions of the three strings are T_i , $i = 1, 2, 3$, the angles are uniquely determined by

$$\theta_1^t = \cos^{-1} \frac{T_2^2 + T_3^2 - T_1^2}{2T_2T_3}, \quad 0 < \theta_1^t < \pi, \quad (32)$$

and similar equations for θ_2^t and θ_3^t . These are equivalent to

$$T_1 : T_2 : T_3 = \sin \theta_1^t : \sin \theta_2^t : \sin \theta_3^t, \quad \theta_1^t + \theta_2^t + \theta_3^t = \pi. \quad (33)$$

Unlike the relation between θ_i^f and θ_i^r , θ_i^t is not a function of only the single angle θ_i^f with the same index i but a function of a set of the angles $(\theta_1^f, \theta_2^f, \theta_3^f)$. Because the sum of the three flux angles are π or 2π , only two of them are independent. Let us represent θ_1^t as a function of θ_2^f and θ_3^f , and denote it by $\theta_1^t = \tau(\theta_2^f, \theta_3^f)$. The other two angles are similarly given by $\theta_2^t = \tau(\theta_3^f, \theta_1^f)$ and $\theta_3^t = \tau(\theta_1^f, \theta_2^f)$ with the same function τ .

For the MN case, (33) reduces to a simple relation $\sin \theta_i^t = \sin \theta_i^f$. Even in this case, we cannot determine θ_i^t from only a single angle θ_i^f because there are two solutions $\theta_i^t = \theta_i^f$ and $\theta_i^t = \pi - \theta_i^f$. These two solutions correspond to the two possible values π and 2π of the total flux angle $\theta_{\text{tot}}^f = \sum_{i=1}^3 \theta_i^f$, respectively. These two cases can be unified into one equation

$$\theta_3^t = \tau(\theta_1^f, \theta_2^f) = |\pi - \theta_1^f - \theta_2^f|. \quad (34)$$

Let us proceed to discussion of four-string junctions. We assume the four external strings are on a plane. Let us label the external strings in the counter-clockwise order by 1, 2, 3 and 4, and denote the angle made by strings i and $i+1$ by $\theta_{i,i+1}$. ((a) in Figure 3) (The labels of strings are defined mod 4.) The sum

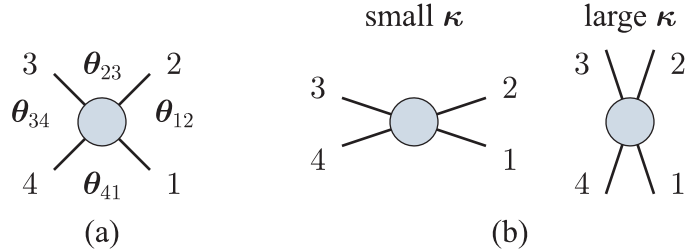


Figure 3: A junction with four external strings.

of these four angles is 2π , and only three of them are independent. If the flux angles $(\theta_1^f, \theta_2^f, \theta_3^f, \theta_4^f)$ of four branches are given, the tensions are determined by the formula above, and the balance of these four tensions imposes two conditions on the angles $\theta_{i,i+1}$. These conditions leave one degree of freedom unfixed. Let us define a parameter κ parameterizing the unfixed freedom. One useful choice is

$$\kappa = \theta_{12} + \theta_{34} = 2\pi - (\theta_{23} + \theta_{41}). \quad (35)$$

If this parameter changes, the junction deforms like (b) in Figure 3.

There are three possible topologies of junctions as shown in Figure 4. For

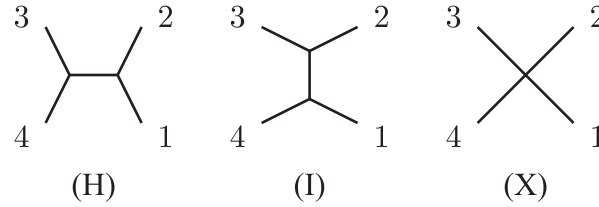


Figure 4: Three topologies of four-string junctions. Two of them include two three-string vertices and the other has one four-string vertex.

junctions of the topologies (H) and (I), which include two three-string vertices, the angles $\theta_{i,i+1}$ are uniquely determined by the flux angles, and the corresponding κ -parameters are given by

$$\kappa_H = 2\pi - \tau(\theta_1^f, \theta_2^f) - \tau(\theta_3^f, \theta_4^f), \quad \kappa_I = \tau(\theta_2^f, \theta_3^f) + \tau(\theta_4^f, \theta_1^f). \quad (36)$$

Let us suppose that there is a junction with the topology (H). This can be in equilibrium if $\kappa = \kappa_H$. If we try to change the κ -parameter by changing the direction of strings, the two vertices move in such a way that the movement compensates the variation of κ . If we try to decrease κ , two vertices move away

from each other to keep the parameter κ unchanged. If we move the strings in the opposite direction, two vertices approach to each other. This compensating mechanism by the movement of vertices works until two vertices coincide. If we continue to move the strings after the coincidence, the topology of the junction intends to change to (I) via (X). Until the moment of the coincidence of two vertices, the κ -parameter is equal to κ_H , and the behavior of the junction after the coincidence depends on the relation between κ_H and κ_I .

If $\kappa_H > \kappa_I$, just as two vertices of (H) meet, the junction changes its topology to (I) and gets unstable, and two vertices separate away rapidly to realize the equilibrium condition $\kappa = \kappa_I$. In this case junctions of the topology (X) are unstable.

If $\kappa_H < \kappa_I$, even after two vertices coincide, the topology does not change to (I), and (X) is stable until κ reaches κ_I . When κ reaches κ_I , the junction finally changes its topology to (I).

When $\kappa_H = \kappa_I$, there is a unique parameter κ which gives stable configurations, and the three topologies can change to each other marginally without changing κ .

To express these behaviors of junctions, it is convenient to define the parameter $\lambda \equiv \kappa_H - \kappa_I$ representing “repulsive force” between two vertices. If λ is positive, two three-string vertices repel each other, and they cannot merge to form a stable four-string vertex. If λ is negative, two vertices attract each other and they are bound into a four-string vertex provided $\kappa_H < \kappa < \kappa_I$.

Which cases happen for junctions in the MN and the KS backgrounds? From (35) and (36), $\lambda = \kappa_H - \kappa_I$ is given by

$$\lambda = 2\pi - \tau(\theta_1^f, \theta_2^f) - \tau(\theta_2^f, \theta_3^f) - \tau(\theta_3^f, \theta_4^f) - \tau(\theta_4^f, \theta_1^f). \quad (37)$$

For the MN solution, the explicit form of λ is

$$\lambda = 2\pi - |\pi - \theta_1^f - \theta_2^f| - |\pi - \theta_2^f - \theta_3^f| - |\pi - \theta_3^f - \theta_4^f| - |\pi - \theta_4^f - \theta_1^f|. \quad (38)$$

We can easily show that $\lambda = 0$ when $\sum_{i=1}^4 \theta_i^f = \pi$ or $\sum_{i=1}^4 \theta_i^f = 3\pi$, and $\lambda > 0$ when $\sum_{i=1}^4 \theta_i^f = 2\pi$.

For the KS solution, although it is difficult to determine the signature of λ analytically, we can numerically check that it is always positive. This implies that planar four-string junctions are always unstable in the KS background.

4 Reduction to lower dimension

In the last section we saw that junctions are described as three-dimensional surfaces in the six-dimensional space spanned by the coordinates $(x, y, z, \theta, \phi, \psi)$. We only consider planar junctions and set $z = 0$. If we ignore the extension along (x, y) -plane, the worldvolume of a D3-brane representing a k -string junction is

an S^3 with k punctures. Each puncture is topologically three-dimensional disc, and corresponds to each branch string. Let us assume that these punctures are located on a large circle of S^3 . In this case the configuration possesses a $U(1)$ symmetry which does not move the large circle. It is convenient to choose S^1 given by $g_{\psi\psi} = 0$ as the fixed large circle so that the $U(1)$ action is a constant shift of the coordinate ψ . General brane configurations with this $U(1)$ symmetry are

$$x = x(\sigma^1, \sigma^2), \quad y = y(\sigma^1, \sigma^2), \quad \theta = \theta(\sigma^1, \sigma^2), \quad \phi = \phi(\sigma^1, \sigma^2), \quad \psi = \sigma^3. \quad (39)$$

Thus we can represent configurations as two-dimensional surfaces in the four-dimensional space with coordinates (x, y, θ, ϕ) .

Instead of the angular coordinates (θ, ϕ) , it is convenient to use (u, v, w) obeying constraints $u^2 + v^2 + w^2 = 1$ and $w \geq 0$. The relations among these coordinates are

$$u = \sin \theta \cos \phi, \quad v = \cos \theta, \quad w = \sin \theta \sin \phi. \quad (40)$$

(Figure 5) If we use (x, y, u, v) as a set of independent coordinates, the target space is $\mathbf{R}^2 \times \mathbf{D}^2$ where \mathbf{R}^2 is spanned by x and y , and \mathbf{D}^2 is the unit disc $u^2 + v^2 \leq 1$ on the (u, v) -plane. The variable $w = \sqrt{1 - u^2 - v^2}$ is treated as a function of u and v . Brane configurations are two-dimensional surfaces embedded in this four-dimensional target space. For example, a confining string solution given in §3 is represented as a band in the four-dimensional space which is a direct product of a chord $v = \cos \theta^r$ on the unit disc and an infinitely long line on the (x, y) -plane.

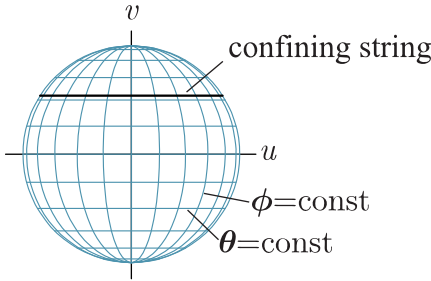


Figure 5: The projection of the hemisphere parameterized by (θ, ϕ) to the unit disc on the (u, v) -plane. The cross-section of a confining string solution is represented as a chord of the unit circle on the (u, v) -plane.

We should redefine the electric flux density as a field on the two-dimensional surface by integrating the flux density D_2 along ψ . We introduce a one-form D'_1 and its dual vector D'^a by

$$D'_1 = \int_{\psi} D_2, \quad D'_1 = \sqrt{\det g_{ab}} \epsilon_{ab} D'^a d\sigma^b, \quad (a, b = 1, 2). \quad (41)$$

The Gauss law constraint satisfied by D'_1 is obtained by integrating the constraint (16) as

$$dD'_1 = 2\pi\rho du \wedge dv. \quad (42)$$

The corresponding integral form is

$$2\pi\rho\theta^f = \oint_C D'_1 - 2\pi\rho \int_A du \wedge dv, \quad (43)$$

where C and A correspond to X and Y in (15), respectively. C is a curve on the surface connecting two boundaries. A is a two-dimensional surface whose boundary consists of C and a curve in the boundary $u^2 + v^2 = 1$ of the four-dimensional target space. To obtain the right hand side of equations (42) and (43), we used

$$\int_{\psi} \omega_3 = 2\pi \sin^2 \theta \sin \phi d\theta \wedge d\phi = 2\pi du \wedge dv. \quad (44)$$

The energy (17) integrated by ψ is

$$E = \int d^2\sigma \sqrt{\det g_{ab}} \sqrt{(2\pi w)^2 + g_{ab} D'^a D'^b}, \quad (a, b = 1, 2). \quad (45)$$

Now the problem which we want to solve is to find a two-dimensional surface in the four-dimensional space (x, y, u, v) and a flux density D'_1 on it which minimize the energy (45) under the constraint (43) imposed on each external confining string.

When we perform a numerical computation to determine a brane configuration, we start from an initial configuration, and look for a configuration with minimum energy by varying the shape of the surface and the flux on it. We can choose any configuration as an initial configuration as long as it satisfies appropriate boundary conditions and (43), and is in the same topology class with the final configuration we want to obtain. One natural choice for a confining string is a D3-brane with a shrank worldvolume, for which the second term of (15) vanishes. It represents a brane before puffed up by the Myers' effect. This is, however, so singular and not appropriate for the numerical computation. Instead we adopt a worldvolume on which the electric flux density vanishes everywhere on the surface. In this case, the constraint (43) requires that the area on the (u, v) -plane enclosed by C and the unit circle $u^2 + v^2 = 1$ should be the same with the flux angle θ^f . The most convenient one satisfying this condition is “wedge configuration” defined as a direct product of a line on the (x, y) -plane and a wedge on the (u, v) -plane shown in Figure 6 (a).

Starting from a wedge configuration with a central angle $2\theta^f$, we can numerically reproduce the corresponding confining string solution represented as a chord on the (u, v) -plane. Its length is determined by θ^r defined in §3. For the MN solution, the two angles θ^f and θ^r are equal to each other. This implies that the distance between the two endpoints of the wedge on the unit circle is the same

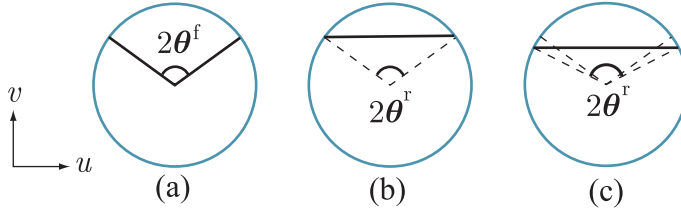


Figure 6: The projections of brane configurations on the (u, v) -plane. (a) is a wedge configuration used as an initial configuration. (b) and (c) are confining string solutions in the MN and the KS backgrounds, respectively.

with that of the chord. ((b) in Figure 6) On the other hand, the distance becomes slightly longer for the KS solution. ((c) in Figure 6)

Wedge configurations are also suitable to construct initial configurations for junctions because it can be pasted just like interaction vertices in Witten's open string field theory[38] as shown in (a) of Figure 7. By varying this initial config-

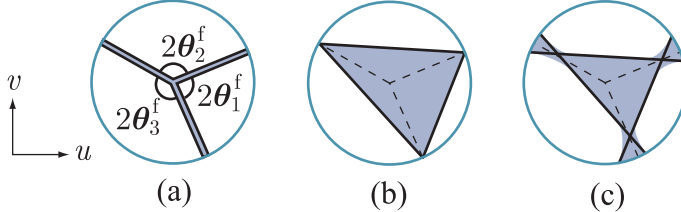


Figure 7: An initial configuration (a) for a three string junction is made of three wedge configurations. After minimizing the energy by varying the configuration, we would obtain junction solutions (b) and (c) for the MN and the KS backgrounds, respectively.

uration and minimizing the energy, we obtain a junction configuration.

In the case of the MN background, the distance between the endpoints of each curve representing each branch string does not change, and the junction solution is expected to be a triangle inscribed in the unit circle on the (u, v) -plane. (Figure 7 (b)) Indeed, the coincidence of the endpoints of the three chords is guaranteed by the relations (49) we will give later. It is important that this triangle is similar to the tension triangle in Figure 2.

For the KS solution, the chords representing asymptotic string solutions are too long to make an inscribed triangle. (Figure 7 (c))

5 Numerical analysis

In this section, we study brane configurations numerically. We start with reconstructing confining string solutions to assess the accuracy of results of the numerical method by comparing them to analytic results given in §3.

We first prepare a wedge configuration with a central angle $2\theta^f$ and a length L as an initial configuration. ((a) in Figure 8). We compute the energy of the surface by means of the triangulation method. The surface is divided into

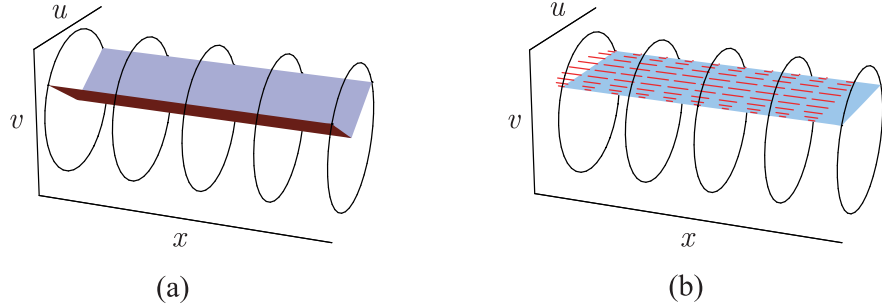


Figure 8: An initial wedge configuration (a) and a numerically generated confining string solution (b). The segments on the worldvolume in (b) represent the flux density.

$2n_{\text{mesh}}^2$ small triangular meshes. The shape of the surface is represented by the positions of sites, and the flux density is treated as link variables. We look for a configuration minimizing the energy by varying these variables with taking account of the Gauss law constraint. The detailed algorithm is given in the appendix. A result for ($\theta^f = \pi/3$, $L = 4$, $b = 1$) is given in Table 2. By

Table 2: A numerical result for the tension of a confining string with $\theta^f = \pi/3$ in the MN solution. The value for $n_{\text{mesh}} \rightarrow \infty$ is obtained by extrapolating the data for $n_{\text{mesh}} = 10, 20, 40$ and 80 with the fitting function $c_0 + c_1 n_{\text{mesh}}^{-2} + c_2 n_{\text{mesh}}^{-4} + c_3 n_{\text{mesh}}^{-6}$.

n_{mesh}	10	20	40	80	∞	exact
$T = E/L$	10.7858	10.85978	10.87722	10.88144	10.88283	10.88280
error	-0.0970	-0.02302	-0.00558	-0.00136	+0.00003	-

comparing this result to the corresponding tension in Table 1, we can estimate the accuracy of the outputs of the numerical analysis. We find a relative error of the order of $\sim 10^{-4}$ for the smallest meshes with $n_{\text{mesh}} \sim 80$. Plotting the error as a function of the typical size of triangles $a = n_{\text{mesh}}^{-1}$, we find that the error is almost proportional to a . (See Figure 9.) The value for $n_{\text{mesh}} = \infty$ ($a = 0$) in Table 2 is obtained by extrapolating the data for finite n_{mesh} with a polynomial of a . This extrapolation gives a very close value to the exact one with a relative error $< 10^{-5}$. So, we shall use the same extrapolation to obtain energies of baryon vertices.

Let $E_{\text{junc}}(L)$ be the energy of a three string junction with the branch length

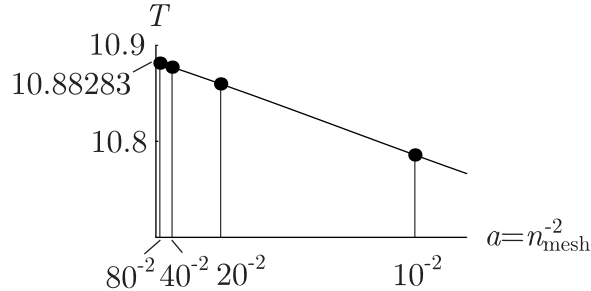


Figure 9: A fitting of numerically generated tensions for different n_{mesh}

L . The contribution from a baryon vertex is defined by

$$E_{\text{vertex}} = \lim_{L \rightarrow \infty} \left(E_{\text{junc}}(\theta_i^f, L) - L \sum_i T(\theta_i^f) \right). \quad (46)$$

However, we cannot in practice numerically compute E_{junc} in the limit $L \rightarrow \infty$. Instead, we use a sufficiently long fixed length beyond which the effect of vertices becomes negligible. We confirm in the following way that $L = 4$ seems to be enough to guarantee a relative accuracy of 10^{-5} . We compute energies of two strings stretched between $x = 0$ and $x = L$ with different lengths $L = 4$ and $L = 8$. The worldvolume of the short and the long strings are made of $2n_{\text{mesh}}^2$ and $4n_{\text{mesh}}^2$ triangles, respectively, so that the areas of triangles become almost the same. The difference from the computation made above to estimate the accuracy is that this time on one boundary at $x = 0$ we impose the fixed boundary condition which prohibit the boundary from changing its shape from a wedge to a straight chord. Thus, the resulting configurations have a wedge-form boundary at $x = 0$, and as x becomes large the shape approaches a string solution. (Figure 10) If the difference of energies of the two branes with different lengths $L = 4$ and

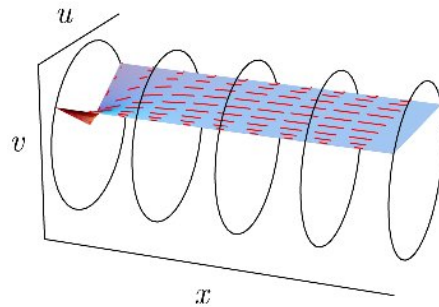


Figure 10: The brane configuration with a boundary on which the fixed boundary condition is imposed.

8 is sufficiently close to the energy of a confining string with a length $4 = 8 - 4$, the configuration has sufficiently approached the string solution around $x \sim 4$,

Table 3: The numerically computed energies of the confining string configurations a fixed boundary at one end. $T(n_{\text{mesh}})$ is the numerically computed tension given in Table 2.

n_{mesh}	10	20	40	80
$E_{L=8}$	87.2002	87.75829	87.88710	87.91770
$E_{L=4}$	44.0562	44.31901	44.37818	44.39194
$(E_{L=8} - E_{L=4})/(8 - 4)$	10.7860	10.85982	10.87723	10.88144
Difference from $T(n_{\text{mesh}})$	+0.0002	+0.00004	+0.00001	+0.00000

and we can use $L = 4$ to compute the energies of baryon vertices. The result of this analysis is given in Table 3, and we certainly confirm that the configuration sufficiently approaches a string solution before x reaches $L = 4$.

Based on these preliminary results, we can finally compute the energies of baryon vertices. The initial configurations are the combination of three wedges pasted like Witten's 3-string vertices ((a) in Figure 11). The directions of three branches of initial configurations on the (x, y) -plane are set as in Figure 2 so that the tensions are balanced. Instead of taking the $L \rightarrow \infty$ limit, we simply use

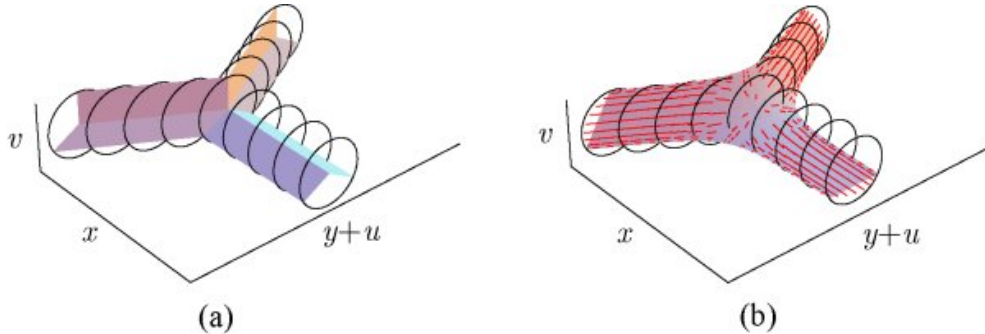


Figure 11: An initial configuration made of three wedge configurations and the corresponding final junction configuration obtained by the numerical method.

$L = 4$, and each branch consists of $2n_{\text{mesh}}^2$ triangles.

We first give results for the KS background in Table 4. Because vertices with more than three branches are unstable, we only give the results for three string vertices. Against the intuitive expectation, the signatures of the baryon vertex energies are negative. The absolute values depend on the ratio of the flux angles, and it seems that the more asymmetric flux angles are, the closer to zero the energy is. This behavior comes up to our expectation because in the limit where one of the flux angle vanishes the junction becomes a confining string configuration and the energy of the vertex goes to zero.

Results for vertex energies in the MN background are more interesting. As shown in Table 5, the ratios of vertex contributions to the total energies are

Table 4: The energies of baryon vertices in the KS solution. E_{junc} is the energy of a whole junction with branch length $L = 4$. E_0 represents the contribution of branches computed by $E_0 = \sum_{i=1}^3 LT(\theta_i^f)$. The energy of a vertex is defined by $E_{\text{vertex}} = E_{\text{junc}} - E_0$. The shaded numbers are final results obtained by the extrapolation.

$\theta_1^f : \theta_2^f : \theta_3^f$	n_{mesh}	10	20	40	80	∞
4 : 4 : 4	E_{junc}	131.014	131.8324	132.0261	132.0731	132.0886
$E_0 = 132.5661$	E_{vertex}	-1.552	-0.7337	-0.5400	-0.5130	-0.4775
3 : 4 : 5	E_{junc}	128.126	128.9356	129.1274	129.1740	129.1894
$E_0 = 129.6061$	E_{vertex}	-1.480	-0.6705	-0.4787	-0.4321	-0.4167
2 : 5 : 5	E_{junc}	122.473	123.3349	123.5420	123.5927	123.6095
$E_0 = 123.8908$	E_{vertex}	-1.418	-0.5559	-0.3488	-0.2981	-0.2813

smaller than 10^{-5} . This strongly suggests that the energies of baryon vertices exactly vanish regardless of the flux angles. In other words, the energy of a

Table 5: The energies of baryon vertices in the MN solution. E_{junc} , E_0 , and E_{vertex} are defined in the same way with those in Table 4. The shaded numbers are final results obtained by the extrapolation.

$\theta_1^f : \theta_2^f : \theta_3^f$	n_{mesh}	10	20	40	80	∞
4 : 4 : 4	E_{junc}	129.584	130.3545	130.5356	130.5794	130.5939
$E_0 = 130.5936$	E_{vertex}	-1.010	-0.2391	-0.0580	-0.0142	+0.0003
3 : 4 : 5	E_{junc}	126.616	127.3866	127.5686	127.6127	127.6273
$E_0 = 127.6270$	E_{vertex}	-1.011	-0.2404	-0.0584	-0.0143	+0.0003
2 : 5 : 5	E_{junc}	121.116	121.9670	122.1716	122.2217	122.2383
$E_0 = 122.2382$	E_{vertex}	-1.122	-0.2712	-0.0666	-0.0165	+0.0001

junction is obtained by summing up the contribution of each branch given as the product of its tension and its length on the (x, y) -plane. We also give another result for a stable planar four-string vertex. It seems consistent with a vanishing vertex energy again.(Table 6)

Before ending this section, let us confirm that junction configurations in the MN background have the asymptotic forms suggested in §3, which are represented as triangles on the (u, v) -plane. The projection of a numerically generated junction on (u, v) -plane is shown in Figure 12, and it certainly seems to be a triangle as we expected.

Table 6: The energy of a planar four-string vertex with $\theta_i^f = \pi/4$. E_{junc} , E_0 , and E_{vertex} are defined in the same way with those in Table 4 and 5. The shaded number is the final result obtained by the extrapolation.

$\theta_1^f : \theta_2^f : \theta_3^f : \theta_4^f$	n_{mesh}	10	20	40	80	∞
3 : 3 : 3 : 3	E_{junc}	141.329	141.9459	142.1079	142.1537	142.1695
$E_0 = 142.1723$	E_{vertex}	-0.843	-0.2264	-0.0644	-0.0186	-0.0028

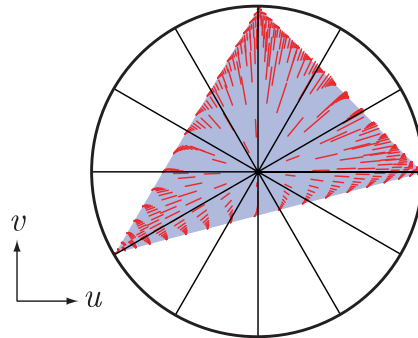


Figure 12: A three-string junction configuration in the MN background projected on the (u, v) -plane

6 Analytic proof

As we saw in the last section, the numerical results for junctions in the MN background strongly suggest that baryon vertices do not contribute to the energies of junctions at all. This property is the same with supersymmetric junctions consisting of (p, q) -strings. [39, 40, 41, 42, 43, 44, 45] This fact for (p, q) -junctions is proven by dualizing junctions to membrane configurations in M-theory[44]. From this viewpoint, junctions are represented as two-dimensional smooth surfaces embedded in a four-dimensional space $\mathbf{R}^2 \times \mathbf{T}^2$. Let (X, Y) and (U, V) be the orthogonal coordinates in \mathbf{R}^2 and \mathbf{T}^2 , respectively. We combine them into two complex coordinates $Z_1 = X + iU$ and $Z_2 = Y + iV$. Then, a surface in this space is represented by a function $Z_2 = F(Z_1, \bar{Z}_1)$. It is known that if we require a brane configuration to be supersymmetric, the function F should be holomorphic[44, 45]. This fact is crucial for the proof of the disappearance of the energies of vertices[44].

Brane configurations in the MN background have a similar property. As we have seen, they are described as two-dimensional smooth open surfaces in the four-dimensional space $\mathbf{R}^2 \times \mathbf{D}^2$ with coordinates (x, y, u, v) . Let us define complex coordinates $z_1 = x + iu$ and $z_2 = y + iv$ in imitation of the (p, q) -junction case. A surface can be represented by an equation $z_2 = f(z_1, \bar{z}_1)$. Far from the vertex, each branch of the surface asymptotically approaches a confining string

solution, which is represented by

$$y = a_i x + b_i, \quad u = c_i v + d_i, \quad (47)$$

where i is the label of the branch. When we rewrite these relations in terms of complex variables z_1 and z_2 , the function f is holomorphic if the coefficients a_i and c_i are the same. We can always set $a_i = c_i$ for one i by a rotation of the coordinates u and v . Furthermore, due to the similarity of the triangles in Figure 2 and Figure 7, the relation $a_i = c_i$ can be achieved for all i at the same time. Therefore, the function f becomes holomorphic in the asymptotic part of all the branches. We call this property “asymptotic holomorphy”. In terms of real variables, the holomorphy of the function f is represented by the Cauchy-Riemann relations:

$$\left(\frac{\partial v}{\partial u} \right)_x = \left(\frac{\partial y}{\partial x} \right)_u, \quad \left(\frac{\partial y}{\partial u} \right)_x = - \left(\frac{\partial v}{\partial x} \right)_u. \quad (48)$$

In fact, the second equation in (48) is vacuous as a condition for asymptotic shapes of surfaces. Because we are considering brane configurations which asymptotically approach confining string solutions, the asymptotic forms are always represented by the two factorized equations in (47). In this case, the second equation in (48) reduces to a trivial relation $0 = 0$.

This asymptotic holomorphy can be used to check the stability of four-string vertices. Under the assumption of the coincidence of endpoints of chords, the relation $\theta^f = \theta^t$ for the MN background means that k chords representing branches of a k -string junction make a k -gon inscribed in the unit circle on the (u, v) -plane. For four-string junctions, there are three cases distinguished by $\theta_{\text{tot}}^f \equiv \sum_{i=1}^4 \theta_i^f$. If $\theta_{\text{tot}}^f = \pi$ or 3π the squares defined on the (u, v) -plane in this way are similar to the squares made of four tension vectors of four external strings just like in the case of three-string junctions. However, if $\theta_{\text{tot}}^f = 2\pi$, the inscribed squares are twisted and cannot be similar to the tension squares. ((a) in Figure 13) In this

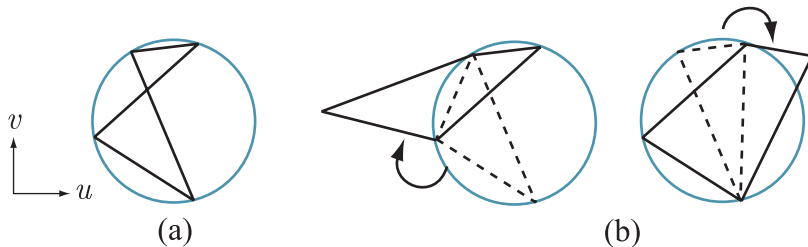


Figure 13: (a) A twisted square for $\theta_{\text{tot}}^f = 2\pi$. (b) Two ways of unfolding.

case, we obtain squares similar to the tension squares by unfolding the twisted squares. Two ways of unfolding correspond to two different topologies (H) and (I), which cannot be deformed smoothly to each other. ((b) in Figure 13) From

these facts, we conclude that a four-string vertex is stable only if it satisfies the asymptotic holomorphy condition, which is equivalent to the similarity of the tension squares and the inscribed squares on the (u, v) -plane.

The asymptotic holomorphy relations are not enough to compute the energies of baryon vertices. We need to find some relations which hold everywhere on branes. One possibility is that the asymptotic holomorphy can be extended to the whole worldvolume as they are. Disappointingly, however, we can show that it is not the case by checking numerically generated junction solutions. Instead, we can show that the following “modified Cauchy-Riemann relations” are satisfied everywhere on branes.

$$\left(\frac{\partial v}{\partial u}\right)_x = \left(\frac{\partial y}{\partial x}\right)_u, \quad w \left(\frac{\partial y}{\partial u}\right)_x = -\frac{1}{w} \left(\frac{\partial v}{\partial x}\right)_u. \quad (49)$$

Note that these relations do not conflict with the asymptotic holomorphy relations (48), but guarantee them. Because the relation between (x, u) and (y, v) is factorized as (47) in asymptotic regions, the second relation in (49) becomes trivial as the second relation in (48).

One way to find the relations (49) is the following. We start with deciding the ansatz for the flux density. Let us look at Figure 12. The radial pattern of the flux in it implies that $(D^u, D^v) \propto (u, v)$. The proportional factor can be determined by the Gauss law constraint (42), and we obtain

$$D'_1 = 2\pi(u dv - v du), \quad D'^a = \frac{2\pi}{\sqrt{\det g_{ab}}} u^a, \quad (50)$$

where $u^a = (u, v)$, and we use the static coordinates $\sigma^a = u^a$. Then, by substituting this ansatz to the energy (45), we obtain

$$E = 2\pi \int d^2\sigma \sqrt{\det \hat{g}_{ab}}, \quad (51)$$

with the effective induced metric \hat{g}_{ab} defined by

$$\hat{g}_{ab} = \frac{1}{w} \delta_{ab} + w X_a^i X_b^i, \quad (52)$$

where $X^i = (x, y)$ and $X_a^i = \partial X^i / \partial u^a$. The expression (51) implies that the two-dimensional surfaces can be treated as Nambu-Goto type branes in the background with the effective metric

$$\widehat{ds}^2 = \frac{1}{w} (du^2 + dv^2) + w(dx^2 + dy^2). \quad (53)$$

Thus, it is quite natural to replace du , dv , dx , and dy in the Cauchy-Riemann relations (48) by $w^{-1/2}du$, $w^{-1/2}dv$, $w^{1/2}dx$, and $w^{1/2}dy$, respectively. In this

way, we discovered the relations (49), which take the place of the holomorphy for (p, q) -string junctions.

Let us prove that the equations of motion are automatically satisfied if the shape of a brane satisfies the modified Cauchy-Riemann relations (49), and the flux density on it is given by the ansatz (50). The equation of motion for X^i obtained from the energy (51) is

$$\partial_a \left(\sqrt{\det \hat{g}_{ab}} w \hat{g}^{ab} X_b^i \right) = 0. \quad (54)$$

In order to obtain the equation of motion for the gauge field, we should use the action (45), to which the ansatz (50) has not been applied. With variations in the form $\delta D^a = (1/\sqrt{g})\epsilon^{ab}\partial_b\phi$, which do not violate the constraint (42), we obtain the Maxwell's equation for the electric field strength E_a

$$\epsilon^{ab}\partial_a E_b = 0, \quad (55)$$

where the relation between E_a and D^a is

$$E_a = \frac{g_{ab}D^a}{\sqrt{(2\pi w)^2 + g_{ab}D^aD^b}}. \quad (56)$$

This can be rewritten by the ansatz (50) as

$$E_a = \frac{g_{ab}u^b}{\sqrt{\det \hat{g}_{ab}}} = \frac{\hat{g}_{ab}u^b}{w\sqrt{\det \hat{g}_{ab}}}. \quad (57)$$

To show that equations of motion (54) and (55) hold, we first rewrite the relations (49) in terms of the functions $x(u, v)$ and $y(u, v)$. By using the chain rule for partial derivatives, we obtain

$$x_u + y_v = 0, \quad x_u y_v - y_u x_v = \frac{1}{w^2}, \quad (58)$$

or equivalently,

$$\text{tr } X_a^i = 0, \quad \det X_a^i = \frac{1}{w^2}. \quad (59)$$

(When we use subscripts to represent derivatives, the independent variables are always u and v .) By using these relations, the effective metric (52) becomes

$$\hat{g}_{ab} = w(X_a^i X_b^i + \delta_{ab} \det X_a^i) = w(x_v - y_u) \begin{pmatrix} -y_u & -y_v \\ x_u & x_v \end{pmatrix}, \quad (60)$$

and its determinant is

$$\det \hat{g}_{ab} = (x_v - y_u)^2. \quad (61)$$

With the help of (60) and (61), we can easily show that the equations of motion (54) and (55) are certainly satisfied.

Although we have shown that the modified Cauchy-Riemann relations (49) and the ansatz (50) guarantee that brane configurations satisfy the equations of motion (54) and (55), the converse is not true. There exist solutions of equations of motion which do not satisfy the modified Cauchy-Riemann relations and the D -field ansatz. An example of such a configuration is the deformed baryon configuration given in [46]. Such configurations, however, do not approach confining string solutions asymptotically, and the existence of them does not spoil the arguments in this section.

Now, we are ready to prove the disappearance of energies of baryon vertices analytically. From (51) and (61), the energy $E_{\text{junc}}(L)$ defined above (46) is given by

$$E_{\text{junc}}(L) = 2\pi \int_J dudv |x_v - y_u| = 2\pi \left| \oint_{\partial J} (xdu + ydv) \right|, \quad (62)$$

where J is the region on a junction worldvolume determined by $x^2 + y^2 \leq L^2$. Before using the Stokes' theorem in (62), the absolute value should be moved out of the integral. This is possible because it is shown from (58) that $x_v - y_u$ never vanishes on the worldvolume. The boundary ∂J consists of two kinds of boundaries, which we call A-boundaries (solid lines in Figure 14) and B-boundaries (dashed lines in Figure 14). The A-boundaries are edges of the surface on the boundary $u^2 + v^2 = 1$ of the target space. The B-boundaries arise due to the cut off $x^2 + y^2 = L$. The A-boundaries are mapped to apices of the triangle when

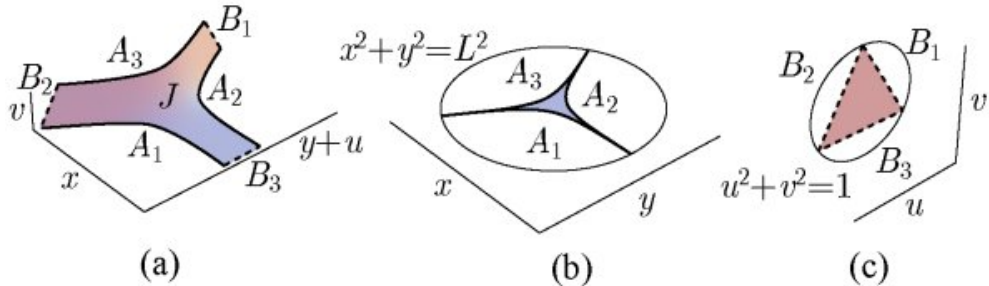


Figure 14: (a) J and its boundary. (b) The projection to the (x, y) -plane. (c) The projection to the (u, v) -plane.

they are projected on the (u, v) -plane, and the coordinates u and v are constants on them. Therefore, A-boundaries do not contribute to the contour integral in (62). Thus, we only need to consider integral on the B-boundaries. If L is sufficiently large, each B-boundary is mapped to a point by the projection to the (x, y) -plane. Let (x_i, y_i) be the point corresponding to the i -th B-boundary B_i . These are on the circle $x^2 + y^2 = L^2$, and we can put

$$(x_i, y_i) = L(\alpha_i, \beta_i), \quad (\alpha_i^2 + \beta_i^2 = 1), \quad (63)$$

where (α_i, β_i) is a unit vector representing the direction of the i -th branch on the (x, y) -plane. If we project B-boundaries to the (u, v) -plane, they are mapped

to sides of the triangle when L is sufficiently large. Due to the similarity between this triangle and the tension triangle, which is guaranteed by the modified Cauchy-Riemann relations (49), the integration measure (du_i, dv_i) on B_i can be represented as

$$(du_i, dv_i) = \pm(\alpha_i, \beta_i)dl_i, \quad (64)$$

where the signature depends on the orientation of the contour, and dl_i is the infinitesimal length on the i -th side of the triangle on the (u, v) -plane. Combining (63) and (64), we obtain the following expression for the energy of a junction.

$$E_{\text{junc}} = 2\pi \sum_i L \int_{B_i} dl_i = 2\pi \sum_i L \times 2 \sin \theta_i^f = \sum_i LT(\theta_i^f). \quad (65)$$

We used the fact that the integral $\int_{B_i} dl_i$ gives the length of the i -th side of the triangle $2 \sin \theta_i^f$, and the tension formula (31) for the MN background. The result (65) means that the energy of a junction is given as the sum of the energies of the branches, and that there is no vertex contribution.

Now we can answer the question raised at the end of §2. Although the expression (21) seemingly depends on g_{str} , which has no counterpart in the boundary field theory of the MN solution, $\tilde{E}_{\text{vertex}}$ in the right hand side is actually zero, and energies of baryon vertices in fact are independent of g_{str} .

7 Conclusions

In this paper, we investigated string junctions in $\mathcal{N} = 1$ supersymmetric gauge theories in the context of the gauge/gravity correspondence. We used the Maldacena-Núñez and the Klebanov-Strassler solutions as gravity duals of confining gauge theories.

In §3 we studied the balance of the tensions for three-string junctions and planar four-string junctions. We found that four-string vertices are stable only in the case of $\theta_{\text{tot}}^f = \pi$ or 3π in the MN solution. Planar four-string vertices in the KS solution are always unstable. It may be interesting to generalize this consideration to non-planar junctions.

In §5 we numerically computed the energies of baryon vertices, and found that the energies are negative in the KS case while in the MN case it almost vanishes. The disappearance of the energies strongly suggests that the brane configurations in the MN background possess some analytic structure which guarantees the vanishing energies. Indeed, we discovered relations similar to the Cauchy-Riemann relations for holomorphic surfaces. With the help of these relations, we analytically proved the disappearance of the energies of baryon vertices.

We should emphasize that our analysis given in this paper is classical. As we mentioned in §3, the existence of confining strings breaks all the supersymmetries. Thus, there is no mechanism to control quantum corrections, and our results can

be justified only in the limit with large N and large $N g_{\text{str}}$, in which the background curvature is small compared to the string scale and the Plank scale.

In order to investigate realistic baryons in non-supersymmetric QCD, we have to use different gravity backgrounds. For example, we can use an AdS Schwarzschild black hole[4, 47]. Because the IR geometry of this solution has similar structure to the KS and the MN solutions, we can study junction configurations in it in a similar way to what we used in this paper.

Only brane configurations embedded in the IR geometry were discussed in this paper. They can be used for highly-excited baryons in which the endpoints of strings separate from each other. To analyze ground-state baryons, we should consider different kind of brane configurations which consist of a baryon vertex and only one external string going up along the r direction to flavor branes. The external string in this case represents coincident quarks. It is important to check whether such branes are stable, and if so, to investigate their energies and excitations.

Other than what we mentioned above, there are many interesting problems associated with brane constructions of hadrons. We hope to return to these issues in the near future.

Acknowledgements

I would like to thank M. Bando and A. Sugamoto for motivating me to do this work. I also thank F. Koyama, H. Ooguri, S. Sugimoto and M. Tachibana for valuable discussions. This work is supported in part by Grant-in-Aid for the Encouragement of Young Scientists (#15740140) from the Japan Ministry of Education, Culture, Sports, Science and Technology, and by Rikkyo University Special Fund for Research.

A Appendix

A.1 Treatment of flux on triangulated surfaces

The purpose of this section is to explain how to discretize branes with flux on them and how to vary variables with keeping the Gauss law constraint.

To compute the energy of a D3-brane, which is represented in (45) as an integral on a two-dimensional surface, we triangulate the surface. We label sites by i, j, k, \dots and each oriented link by two labels representing its two ends. The functions $X^I(\sigma^a)$ describing the shape of the surface are replaced by variables on sites $X_i^I = (x_i, y_i, u_i, v_i, w_i)$ with constraints $u_i^2 + v_i^2 + w_i^2 = 1$ and $w_i \geq 0$ imposed. To represent flux density, we use link variables

$$\phi_{ij} \equiv \int_i^j D'_1, \quad (66)$$

where the integral is carried out along the link ij . This represents the amount of flux flowing across the link ij . We define the orientation in such a way that if the arrow from site i to j is upward, ϕ_{ij} represents the flux passing the link ij from the left to the right. By definition

$$\phi_{ij} = -\phi_{ji}. \quad (67)$$

The area of a triangle ijk is denoted by s_{ijk} . (Figure 15) This area is a real

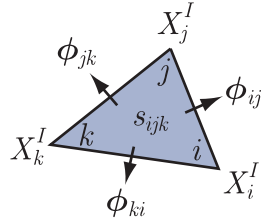


Figure 15: The triangle ijk . X_i^I denotes the coordinate of the vertex i . ϕ_{ij} represents the flux flowing across the link ij . The area of the triangle ijk is denoted by s_{ijk} .

positive number. We also define s'_{ijk} as the area of a triangle ijk projected on the (u, v) -plane. This takes both positive and negative values according to the orientation of the triangle. s_{ijk} and s'_{ijk} are easily represented as functions of variables X_i^I , X_j^I and X_k^I .

Given the variables X_i^I and ϕ_{ij} , the energy of the D3-brane is obtained by the discretized version of the energy (45)

$$E = \sum_{\text{triangles}} s_{ijk} \sqrt{(2\pi w_{ijk})^2 + \sum_I (D'_{ijk}^I)^2}, \quad (68)$$

where w_{ijk} is the w -component of the center of mass $X_{ijk}^I = (X_i^I + X_j^I + X_k^I)/3$ of the triangle ijk , and D'_{ijk}^I is the push-forward of the electric flux density to the five-dimensional space (x, y, u, v, w) , which is given by

$$D'_{ijk}^I = \frac{1}{2s_{ijk}} \{ \phi_{jk}(X_i^I - X_{ijk}^I) + \phi_{ki}(X_j^I - X_{ijk}^I) + \phi_{ij}(X_k^I - X_{ijk}^I) \}. \quad (69)$$

A discretized version of the Gauss law constraint is

$$\phi_{ij} + \phi_{jk} + \phi_{ki} = 2\pi\rho s'_{ijk}. \quad (70)$$

In order to search for a configuration which minimizes the energy, we should vary variables X_i^I and ϕ_{ij} without violating this Gauss law constraint.

There are two kinds of variations. Variations of ϕ_{ij} with fixed X_i^I are generated by the following variation for each site i .

$$\phi_{ji} \rightarrow \phi_{ji} + c, \quad j \in \text{Adj}(i). \quad (71)$$

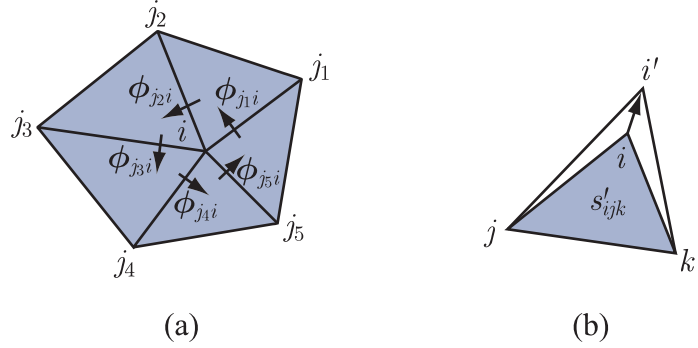


Figure 16: (a) A variation changing the rotation of the electric flux density around i with keeping the Gauss law constraint. (b) If a site i moves to i' , the projected areas of triangles including the site change.

$\text{Adj}(i)$ means the set of all the sites adjoining the site i . This variation changes the rotation of the flux density around the site i . ((a) in Figure 16)

The other kind of variations are what change X_i^I . Even when we vary the variables X_i^I , we should take account of the Gauss law constraint (70) because variations of X_i^I change charges in triangles. If the position of a site i moves from X_i^I to $X_{i'}^I = X_i^I + \delta X_i^I$, the projected area s'_{ijk} of the triangle ijk is changed by $s'_{jii'} - s'_{kii'}$. ((b) in Figure 16) To keep the Gauss law constraint (70), we should change the flux variables at the same time by

$$\phi_{ki'} = \phi_{ki} - 2\pi\rho s'_{kii'}, \quad k \in \text{Adj}(i). \quad (72)$$

Any continuous deformations can be generated by these two kinds of variations (71) and (72).

References

- [1] J. M. Maldacena, “*The Large N Limit of Superconformal Field Theories and Supergravity*”, *Adv.Theor.Math.Phys.* **2** (1998) 231-252; *Int.J.Theor.Phys.* **38** (1999) 1113-1133, [hep-th/9711200](#).
- [2] S. S. Gubser, I. R. Klebanov, A. M. Polyakov, “*Gauge Theory Correlators from Non-Critical String Theory*”, *Phys.Lett.* **B428** (1998) 105-114, [hep-th/9802109](#).
- [3] E. Witten, “*Anti De Sitter Space And Holography*”, *Adv.Theor.Math.Phys.* **2** (1998) 253-291, [hep-th/9802150](#).
- [4] E. Witten, “*Anti-de Sitter Space, Thermal Phase Transition, And Confinement In Gauge Theories*”, *Adv.Theor.Math.Phys.* **2** (1998) 505-532, [hep-th/9803131](#).

- [5] D. J. Gross, H. Ooguri, “*Aspects of Large N Gauge Theory Dynamics as Seen by String Theory*”, Phys.Rev. **D58** (1998) 106002, [hep-th/9805129](#).
- [6] C. Csaki, H. Ooguri, Y. Oz, J. Terning, “*Glueball Mass Spectrum From Supergravity*”, JHEP **9901** (1999) 017, [hep-th/9806021](#).
- [7] H. Ooguri, H. Robins, J. Tannenhauser, “*Glueballs and Their Kaluza-Klein Cousins*”, Phys.Lett. **B437** (1998) 77-81, [hep-th/9806171](#).
- [8] A. Karch, E. Katz, N. Weiner, “*Hadron Masses and Screening from AdS Wilson Loops*”, Phys.Rev.Lett. **90** (2003) 091601, [hep-th/0211107](#).
- [9] M. Kruczenski, D. Mateos, R. C. Myers, D. J. Winters, “*Meson Spectroscopy in AdS/CFT with Flavour*”, JHEP **0307** (2003) 049, [hep-th/0304032](#).
- [10] T. Sakai, J. Sonnenschein, “*Probing Flavored Mesons of Confining Gauge Theories by Supergravity*”, JHEP **0309** (2003) 047, [hep-th/0305049](#).
- [11] J. Babington, J. Erdmenger, N. Evans, Z. Guralnik, I. Kirsch, “*Chiral Symmetry Breaking and Pions in Non-Supersymmetric Gauge/Gravity Duals*”, Phys.Rev. **D69** (2004) 066007, [hep-th/0306018](#).
- [12] E. Schreiber, “*Excited Mesons and Quantization of String Endpoints*”, [hep-th/0403226](#).
- [13] S. Hong, S. Yoon, M. J. Strassler, “*On the Couplings of Vector Mesons in AdS/QCD* ”, [hep-th/0409118](#).
- [14] M. Kruczenski, L. A. P. Zayas, J. Sonnenschein, D. Vaman “*Regge Trajectories for Mesons in the Holographic Dual of Large- N_c QCD*”, [hep-th/0410035](#).
- [15] E. Witten, “*Baryons And Branes In Anti de Sitter Space*”, JHEP **9807** (1998) 006, [hep-th/9805112](#).
- [16] A. Brandhuber, N. Itzhaki, J. Sonnenschein, S. Yankielowicz, “*Baryons from Supergravity*”, JHEP **9807** (1998) 020, [hep-th/9806158](#).
- [17] Y. Imamura, “*Supersymmetries and BPS Configurations on Anti-de Sitter Space*”, Nucl.Phys. **B537** (1999) 184-202, [hep-th/9807179](#).
- [18] C. G. Callan, A. Guijosa, K. G. Savvidy, “*Baryons and String Creation from the Fivebrane Worldvolume Action*”, Nucl.Phys. **B547** (1999) 127-142, [hep-th/9810092](#).
- [19] D. Berenstein, C. P. Herzog, I. R. Klebanov, “*Baryon Spectra and AdS/CFT Correspondence*”, JHEP **0206** (2002) 047, [hep-th/0202150](#).

- [20] J. Polchinski, M. J. Strassler, “*Hard Scattering and Gauge/String Duality*”, Phys.Rev.Lett. **88** (2002) 031601, [hep-th/0109174](#).
- [21] J. Polchinski, M. J. Strassler, “*Deep Inelastic Scattering and Gauge/String Duality*”, JHEP **0305** (2003) 012, [hep-th/0209211](#).
- [22] M. Bando, T. Kugo, A. Sugamoto, S. Terunuma, “*Pentaquark Baryons in String Theory*”, Prog.Theor.Phys. **112** (2004) 325-355, [hep-ph/0405259](#).
- [23] T. Nakano et al. (LEPS collaboration), Phys. Rev. Lett. **91** (2003), 012000.
- [24] C. Alt et al. (NA49 collaboration), [hep-ex/0310014](#).
- [25] A. Karch, E. Katz, “*Adding flavor to AdS/CFT*”, JHEP **0206** (2002) 043, [hep-th/0205236](#).
- [26] S. -J. Rey, J. -T. Yee, “*Macroscopic strings as heavy quarks: Large- N gauge theory and anti-de Sitter supergravity*”, Eur.Phys.J. **C22** (2001) 379-394, [hep-th/9803001](#).
- [27] J. M. Maldacena, “*Wilson loops in large N field theories*”, Phys.Rev.Lett.**80** (1998) 4859-4862, [hep-th/9803002](#).
- [28] C. P. Herzog, I. R. Klebanov, “*On String Tensions in Supersymmetric $SU(M)$ Gauge Theory*”, Phys.Lett. **B526** (2002) 388-392, [hep-th/0111078](#).
- [29] R. C. Myers, “*Dielectric-Branes*”, JHEP **9912** (1999) 022, [hep-th/9910053](#).
- [30] J. Maldacena, C. Núñez, “*Supergravity description of field theories on curved manifolds and a no go theorem*”, Int.J.Mod.Phys. **A16** (2001) 822-855, [hep-th/0007018](#).
- [31] J. M. Maldacena, C. Núñez, “*Towards the large N limit of pure $N=1$ super Yang Mills*”, Phys.Rev.Lett. **86** (2001) 588-591, [hep-th/0008001](#).
- [32] I. R. Klebanov, N. A. Nekrasov, “*Gravity Duals of Fractional Branes and Logarithmic RG Flow*”, Nucl.Phys. **B574** (2000) 263-274, [hep-th/9911096](#).
- [33] I. R. Klebanov, M. J. Strassler, “*Supergravity and a Confining Gauge Theory: Duality Cascades and χ SB-Resolution of Naked Singularities*”, JHEP **0008** (2000) 052, [hep-th/0007191](#).
- [34] C. P. Herzog, I. R. Klebanov, P. Ouyang, “*D-Branes on the Conifold and $N=1$ Gauge/Gravity Dualities*”, [hep-th/0205100](#).

- [35] S. S. Gubser, I. R. Klebanov “*Baryons and Domain Walls in an $N = 1$ Superconformal Gauge Theory*”, Phys.Rev. **D58** (1998) 125025, [hep-th/9808075](#).
- [36] I.R. Klebanov, A.A. Tseytlin, “*Gravity Duals of Supersymmetric $SU(N) \times SU(N+M)$ Gauge Theories*”, Nucl.Phys. **B578** (2000) 123-138, [hep-th/0002159](#).
- [37] S. S. Gubser, C. P. Herzog, I. R. Klebanov, “*Symmetry Breaking and Axionic Strings in the Warped Deformed Conifold*”, [hep-th/0405282](#).
- [38] E. Witten, “*Noncommutative Geometry And String Field Theory*”, Nucl.Phys. **B268** (1986) 253.
- [39] J. H. Schwarz, “*Lectures on Superstring and M Theory Dualities*”, Nucl.Phys.Proc.Suppl. **55B** (1997) 1-32, [hep-th/9607201](#).
- [40] O. Aharony, J. Sonnenschein, S. Yankielowicz, “*Interactions of strings and D-branes from M theory*”, Nucl.Phys. **B474** (1996) 309-322, [hep-th/9603009](#).
- [41] K. Dasgupta, S. Mukhi, “*BPS Nature of 3-String Junctions*”, Phys.Lett. **B423** (1998) 261-264, [hep-th/9711094](#).
- [42] A. Sen, “*String Network*”, JHEP **9803** (1998) 005, [hep-th/9711130](#).
- [43] S. -J. Rey, J. -T. Yee, “*BPS Dynamics of Triple (p,q) String Junction*”, Nucl.Phys. **B526** (1998) 229-240, [hep-th/9711202](#).
- [44] M. Krogh, S. Lee, “*String Network from M-theory*”, Nucl.Phys. **B516** (1998) 241-254, [hep-th/9712050](#).
- [45] Y. Matsuo, K. Okuyama, “*BPS Condition of String Junction from M theory*”, Phys.Lett. **B426** (1998) 294-296, [hep-th/9712070](#).
- [46] S. A. Hartnoll, R. Portugues, “*Deforming baryons into confining strings*”, [hep-th/0405214](#).
- [47] S. W. Hawking, D. Page, “*Thermodynamics Of Black Holes In Anti-de Sitter Space*”, Commun. Math. Phys. **87** (1983) 577.